# An eight-year-long low-frequency earthquake catalog for Southern Cascadia

**Ariane Ducellier[1], Kenneth C. Creager[1]**

[1]University of Washington

**Key Points:**

- We establish an eight-year-long low-frequency earthquake catalog for southern Cascadia.
- Families from the subduction zone are mainly active during the big tremor events, with down dip families more active than up dip families.
- LFE activity is sensitive to tidal stress changes.

Corresponding author: Ariane Ducellier, `ducela@uw.edu`

**Abstract**

Low-frequency earthquakes (LFEs) are small magnitude earthquakes, with typical magnitude less than 2, and reduced amplitudes at frequencies greater than 10 Hz relative to ordinary small earthquakes. Their occurrence is often associated with tectonic tremor and slow slip events along the plate boundary in subduction zones and occasionally transform fault zones. They are usually grouped into families of events, with all the earthquakes of a given family originating from the same small patch on the plate interface and recurring more or less episodically in a bursty manner. In this study, we extend the LFE catalog obtained by Plourde et al. (2015) during an episode of high tremor activity in April 2008, to the 8-year period 2004-2011. All of the tremor in the Boyarko et al. (2015) catalog south of 42 degrees North has associated LFE activity, but we have identified several **smaller clusters of LFEs without associated tremor activity**, and extend their catalog forward and backward by a total of about 3 years. As in northern Cascadia, the down-dip LFE families have recurrence intervals several times smaller than the up-dip families. For the April, 2008 Episodic Tremor and Slip event, the best recorded LFE families exhibit a strong tidal Coulomb stress sensitivity starting 1.5 days after the rupture front passes by each LFE family. The southernmost LFE family, which has been interpreted to be on the subduction plate boundary, near the up-dip limit of tremor, has a very short recurrence time. Also, these LFEs tend to occur during times when predicted tidal Coulomb stress is discouraging slip on the plate boundary. Both observations suggest this LFE family may be on a different fault.

## Plain language summary

Low-frequency earthquakes (LFEs) are small magnitude earthquakes, with typical magnitude less than 2, and reduced amplitudes at frequencies greater than 10 Hz relative to ordinary small earthquakes. They are usually grouped into families of events, with all the earthquakes of a given family originating from the same small patch on the plate interface. **LFEs tend to happen in bursts, with dozen of earthquakes occurring within a few days, followed by weeks or months of quiet**. In this study, we extend the LFE catalog obtained by Plourde et al. (2015) to the 8-year period 2004-2011. As in northern Cascadia, the **LFE families located at greater depth (down dip) are more active, with shorter time intervals between two earthquake bursts, than the LFE families located at shallower depth (up dip). Earth tides also have an influence on LFE activity: LFEs are more likely to occur when the stress changes associated with the tides favor shear failure on the plate boundary**.

## 1 Introduction

Tectonic tremor is a weak but persistent shaking of the Earth that has been discovered in many subduction zones and some strike-slip faults throughout the world **(Beroza & Ide, 2011)**. Tremor is observed on seismograms as apparent noise whose amplitude is modulated in time in a similar manner at stations that are dozens of kilometers apart from each other **(Obara, 2002)**. It is characterized by a long (several seconds to many minutes), low amplitude seismic signal, emergent onsets, and an absence of clear impulsive phases. Tremor can be explained as a swarm of low-frequency earthquakes (LFEs) **(Shelly et al., 2007a)**, that is small magnitude earthquakes (M $\sim$ 1) which dominant frequency is clearly low (1-10 Hz) compared with that of ordinary tiny earthquakes (up to 20 Hz). The source of the tremor and the LFEs is located on the plate boundary **(Shelly et al., 2006; Bostock et al., 2012; Audet & Kim, 2016)**, and their focal mechanisms represent shear slip on a low-angle thrust fault dipping in the same direction as the plate interface **(Ide et al., 2007; Bostock et al., 2012; Royer & Bostock, 2014)**. LFEs are usually grouped into families of events, with all the earthquakes of a given fam-

ily originating from the same small patch on the plate interface, and recurring more or less episodically in a bursty manner. **Tens of events are thus recorded within a few hours or days during a burst of LFE activity, followed by weeks or months of quiet, with very few events.** In subduction zones such as Nankai and Cascadia, tectonic tremor and LFE observations are spatially and temporally correlated with slow slip observations **(Rogers & Dragert, 2003; Obara et al., 2004)**. Due to this correlation, these paired phenomena have been called Episodic Tremor and Slip (ETS).

The relatively short recurrence of slow slip and tremor events results in a rich history both in space and time and reveals potential patterns. These event histories have allowed scientists to see complete event cycles, which is typically not possible to explore in traditional earthquake catalogs. However, most of the work on LFEs has been focused on detecting LFEs during periods of high tremor activity, grouping them into families of events, and locating the source of the LFE families. Longer catalogs (several years) have been established for LFE families in Mexico (two-year long catalog by Frank et al. (2014)), the San Andreas Fault (fifteen-year-long catalog by Shelly (2017)), Washington State (five-year-long catalog by Sweet et al. (2019) and two-year-long catalog by Chestler and Creager (2017a, 2017b)), **Vancouver Island (ten-year-long catalog by Bostock et al. (2015))**, New Zealand (eight-year-long catalog by Baratin et al. (2018)), and Japan (twelve-year-long catalog by Nakamura (2017), eight-year-long catalog by Ohta and Ide (2017), **eleven-year-long catalog by Kato and Nakagawa (2020), and Japan Meteorological Agency (JMA) catalog since 1999 (Katsumata & Kamaya, 2003)**). These studies have shown that the recurrence behavior of LFE families varies a lot between seismic regions, and inside the same seismic region. In northern Washington, Sweet et al. (2019) have identified and characterized four different LFE families that span the width of the transition zone in the Cascadia Subduction Zone beneath western Washington State. They found that the LFEs swarm duration, recurrence interval, and event size decrease systematically with increasing depth. On the San Andreas Fault, Shelly (2017)) observed a large diversity of recurrence behaviors among the LFE families, from semicontinuous to highly episodic. Particularly, two families exhibited bimodal recurrence patterns (about 3 and 6 days for the first one, and about 2 and 4 days for the second one). Moreover, he observed an increase in the LFE event rate after the 2004 Parkfield earthquake.

Plourde et al. (2015) have detected LFEs in southern Cascadia during the April 2008 ETS event using seismic data from the EarthScope Flexible Array Mendocino Experiment (FAME). They used a combination of autodetection methods and visual identification to obtain the initial templates. Then, they recovered higher signal-to-noise LFE signals using iterative network cross-correlation. They found that the LFE families on the southern Cascadia Subduction Zone were located above the **plate boundary model of McCrory et al. (2006), with a large distribution of depths (28-47 km). However, they suggested that this may be because the model is biased deep.** Three additional LFE families were found on two strike-slip faults, the Maacama and Bucknell Creek faults, which are part of the San Andreas Fault zone.

When the hard work of detecting LFEs and identifying LFE families has been carried out, and enough (a few hundred) LFEs have been identified for a given family, a template waveform can be obtained by stacking all the waveforms corresponding to all the LFEs identified. Once a template is available, additional LFEs can be found by cross-correlating seismic data with the template, and assuming that an LFE is occurring whenever the value of the cross-correlation is higher than a chosen threshold. The signal-to-noise ratios are low, so LFEs can be best identified by stacking the cross-correlation functions of multiple stations. In this study, we first use the catalog established by Plourde et al. (2015) for the months of March and April 2008 to create templates for the temporary seismic stations of the FAME experiment. We then use these templates to extend the catalog to the whole period when the FAME experiment was running, between July 2007 and June 2009. Next, we use the LFE detections from the 2007-2009 period

115 to create templates for the permanent stations of three seismic networks in northern Cal-
116 ifornia. These new templates allow us to extend the LFE catalog to the period 2004-2011.

## 2 Data

118      We used both seismic data from the temporary EarthScope Flexible Array Men-
119 docino Experiment (FAME) distributed by Incorporated Research Institutions for Seis-
120 mology (IRIS), and seismic data from three permanent seismic networks distributed by
121 the Northern California Earthquake Data Center (NCEDC). The FAME network was
122 installed in northern California between July 2007 and June 2009. The three permanent
123 networks are Berkeley Digital Seismic Network (BK), Northern California Seismic Net-
124 work (NC), and Plate Boundary Observatory Strain and Seismic Data (PB). We used
125 both one-component and three-components seismic stations. Depending on availability,
126 we used channels BHZ, EHZ, HHZ, or SHZ as we are mainly interested in the frequency
127 band 1-10Hz. We restricted ourselves to seismic stations less than 100 kilometers away
128 from the epicenter of an LFE family, as we do not expect to have good signal-to-noise
129 ratio for stations located farther away. The complete list of seismic stations and chan-
130 nels used in this study is given in the Supplementary Material. Figure 1 shows a map
131 of the locations of the LFE families, and of the locations of the seismic stations. We can
132 see that we have a good coverage of the area, and most LFE families are surrounded by
133 several seismic stations.
134      Plourde et al. (2015) have kindly shared their LFE catalog with us. For each of
135 66 LFE families they provided hypocentral locations, lists of stations and channels used
136 to detect LFEs, and the timing of all LFE detections. Plourde et al. (2015) have later
137 reduced the number of LFE families to 37, by grouping together families with many com-
138 mon detections, but we chose to use the initial detections to extend the catalog. Using
139 this dataset, we have created LFE templates for each LFE family and each seismic sta-
140 tion and channel. For a given LFE family, a given station and a given channel, we down-
141 loaded an 80-second-long seismic waveform starting 10 seconds before the LFE detec-
142 tion time, we detrended the data, tapered the first and last 5 seconds of the data with
143 a Hann window, removed the instrument response, bandpassed filter between 1.5 and
144 9 Hz, resampled the data to 20 Hz, and cut the first and last 10 seconds of data to ob-
145 tain a one-minute-long template. We then linearly stacked all the waveforms after nor-
146 malizing each waveform with the root mean square (RMS) to obtain a waveform tem-
147 plate for each station and each channel.

## 3 Method

149      **Our ultimate goal is to obtain an eight-year-long LFE catalog using data**
150 **from permanent seismic networks. The first step is to use the templates from**
151 **Plourde et al. (2015) and the data from the FAME experiment to get an LFE**
152 **catalog for 2007-2009. The second step is to use the 2007-2009 FAME cat-**
153 **alog to make templates for the seismic stations from the permanent networks.**
154 **The third step is to use the new templates and the data from the permanent**
155 **networks to get an LFE catalog for 2004-2011.** We used a matched-filter algorithm
156 to detect LFEs. For a given LFE family, we download one hour of seismic data. Then
157 for each station and each channel, we cross-correlate the one-hour long signal with the
158 one-minute-long template for the given station and channel. We scale the correlation co-
159 efficient by the standard deviation so the value is 1 if the correlation is perfect. As the
160 signal-to-noise ratio of the seismic data is low, we may not see obvious peaks in the cross-
161 correlation signal. However, if we stack the cross-correlation signals for all the channels
162 and all the stations, we can see peaks appearing. Whenever the value of the average cross-
163 correlation is higher than a threshold (we chose a threshold equal to eight times the me-
164 dian absolute deviation of the stacked cross-correlation **as was done by Shelly et al.**
165 **(2007a)**), we inferred that there is an LFE. As two peaks separated by a short period
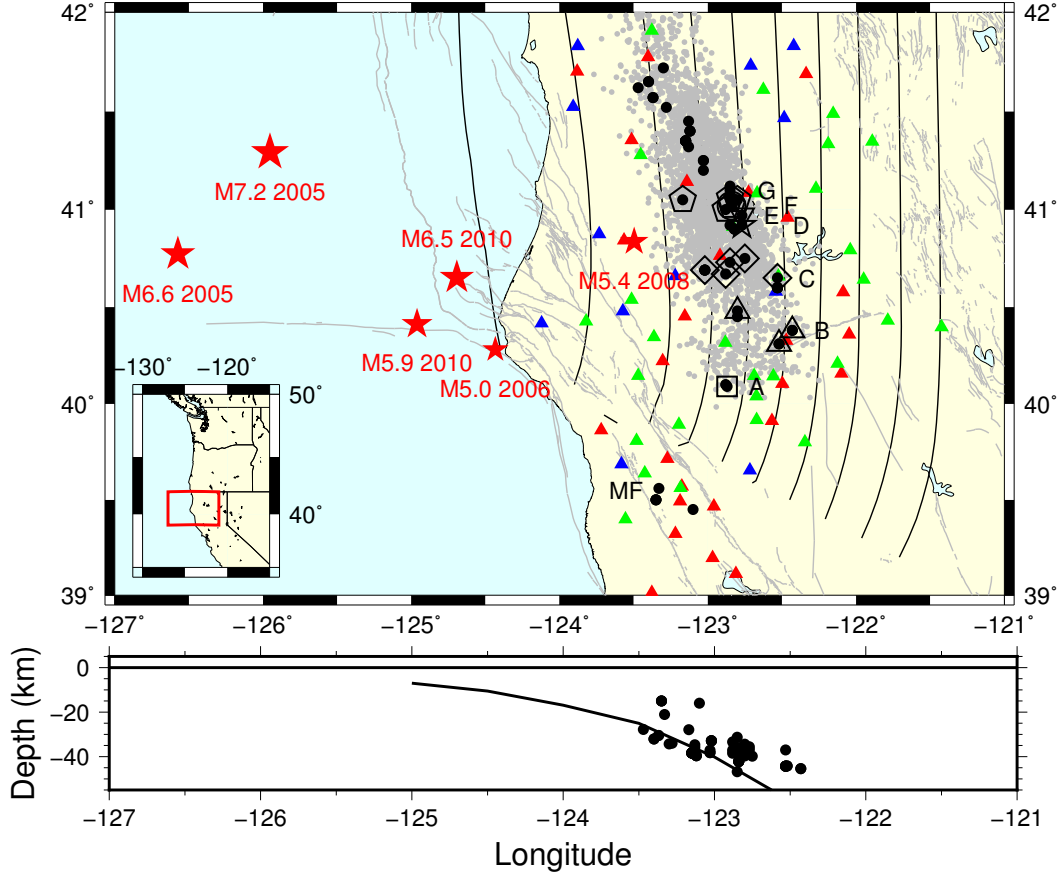
**Figure 1.** Map showing the location of the LFE families (black dots) and the seismic stations used in this study. Red triangles are the stations from the FAME experiment, green triangles are one-component permanent stations, blue triangles are three components permanent stations. Red stars are moderate ($M > 5$) nearby earthquakes. **The plate boundary from McCrory et al. (2006) is contoured at 10-km intervals starting at 10 km depth. The cross section shows the depth of the LFE families (Plourde et al., 2015) and the plate boundary model from McCrory et al. (2006) at latitude 41 N. MF indicates the Maacama Fault.**
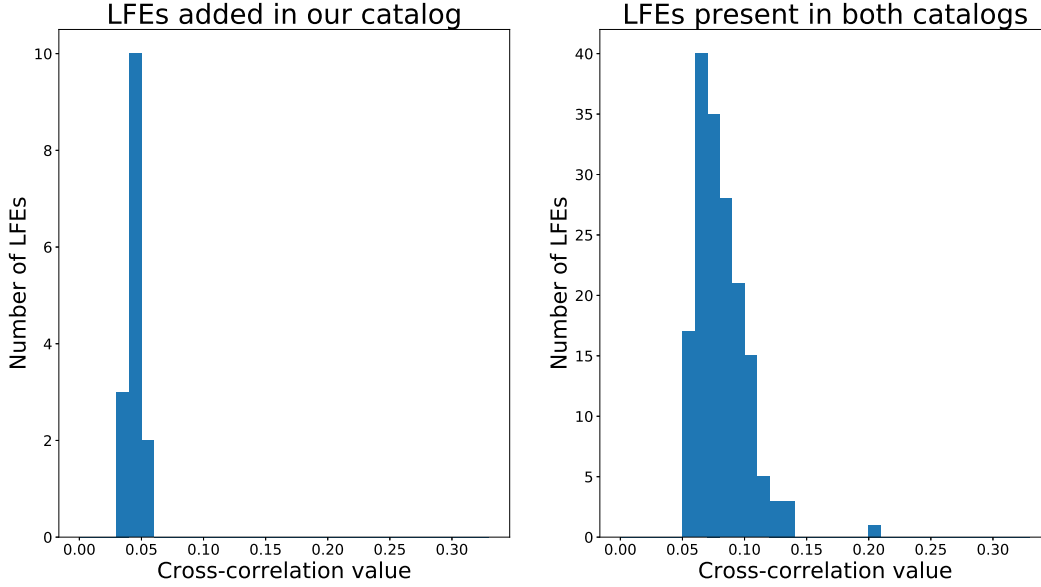
**Figure 2.** Cross-correlation values for LFEs added in the catalog for family E (inverted triangle in Figure 1) (left) and cross-correlation values for LFEs in the original catalog from Plourde et al. (2015) (right). There were no missing LFEs for this family.

of time may actually correspond to the same LFE, we kept only LFEs that are separated by at least one second and, when two LFEs are separated by less than one second, we keep only the one with the higher value of the stacked cross-correlation.

We first looked for LFEs during the months of March and April 2008, which correspond to the period covered by the catalog from Plourde et al. (2015), and compared our detections with the initial detections from the original catalog of 66 families. For 19 families, we recovered all the LFE detections initially present in the Plourde et al. (2015)'s catalog. For 61 families, we recovered more than 90 % of the initial LFE detections. We also added 74 % more LFEs to the **initial number of LFEs in the catalog (when considering all 66 families)**, but most of added LFEs have a low cross-correlation value and may be false detections. Figure 2 shows the cross-correlation values for the LFEs in the original catalog, and for the LFEs that we added to the catalog for family E (inverted triangle in Figure 1).

We then looked for LFEs during the period from July 2007 to June 2009, which correspond to the period when the FAME experiment was operating. Using a threshold equal to eight times the median absolute deviation of the stacked cross-correlation may produce false detections, therefore we filtered the LFE detection times before visualizing the two-year-long catalog. As the number of seismic stations recording may change with time as the stations were progressively installed during Summer and Fall 2007, and then progressively removed during May and June 2009, we kept only LFE detections for which the product of the **stacked** cross-correlation value by the number of **channels** recording at that time is higher than a threshold. **We will explain later in the text how the threshold is chosen**. The threshold is different for each LFE family, **but is constant over time for a given LFE family**. The resulting LFE catalog for the period 2007-2009 is shown in Figure 3. For comparison, we also plotted the tremor detection times from Boyarko et al. (2015). **Filtering the catalog has removed about 84 % of the LFEs, compared to the initial catalog where LFEs were detected using the 8 * MAD threshold for the cross-correlation. As a reference, we plotted in the Supplementary Material (Figure S1) the catalog without filtering the LFEs and the number of channels recording as a function of time.**
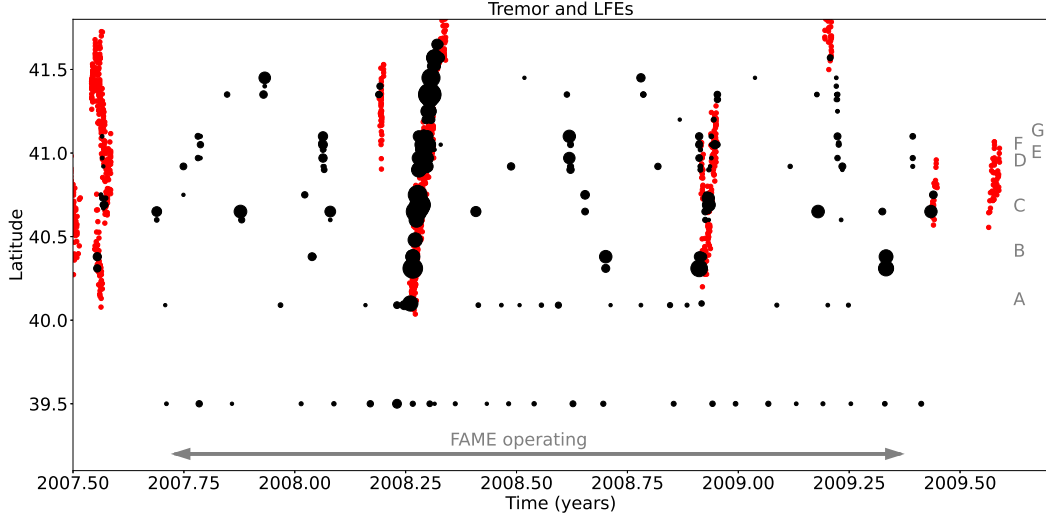
**Figure 3.** LFE and tremor detections as a function of time and latitude. Red dots represent tremor detections from the catalog of Boyarko et al. (2015). Black dots represent days where LFEs are detected for a given LFE family. The size of the black dots are proportional to the number of LFEs detected during this day. The double-headed grey arrow represents the time period when the FAME experiment was operating at full capacity. LFE families south of 40 N latitude are on the San Andreas fault system. For clarity, we do not show the LFEs for the days when there are less than three LFEs.

We note that there is a good spatial and temporal agreement between tremor and LFEs, with LFEs detected during the main tremor episodes. Additional small LFE episodes are also detected between bigger tremor episodes. The LFE families located south on the strike-slip fault from the San Andreas Fault system have much shorter recurrence intervals than the LFE families located on the subduction zone. Additionally, one LFE family located on the southern end of the subduction zone **(family A at 40.09N and 34.9km depth)** has also shorter recurrence intervals than families located farther north, and behaves more similarly to the strike-slip fault families.

We then used the LFE detections from the 2007-2009 catalog to make new templates for the permanent stations of the three seismic networks: Berkeley Digital Seismic Network (BK), Northern California Seismic Network (NC), and Plate Boundary Observatory Strain and Seismic Data (PB). For a given LFE family, we took the 150 LFE detection times with the best cross-correlation value, we downloaded one minute of seismic data around each detection, and linearly stacked the waveforms to obtain the templates. We looked for templates for both one-component stations and three-component stations.

For most families, we find that we can obtain good templates with high signal-to-noise ratio for several stations. Only nine families have four or less seismic stations with good templates. Examples of templates are given in Figure 4 for station WDC and family A (square in Figure 1). To obtain the above catalog, we used one-minute-long templates, which included noise before and after the seismic wave arrivals. To increase the cross-correlation values between the templates and the data, we thus reduced the length of the templates to 25 to 40 seconds, depending on the maximum distance from the source to the stations. **The 2007-2009 FAME catalog has thus been established with cross correlations over one-minute-long templates while the 2004-2011 networks catalog has been established with cross correlations over shorter templates with average duration equal to 30 seconds.** We did not use stations more
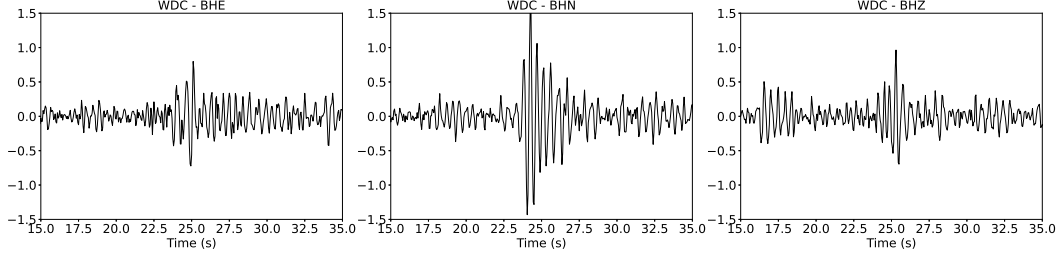
**Figure 4.** Low-frequency earthquake template for station WDC and family A (square in Figure 1) for the three channels BHE, BHN and BHZ (left to right). We can clearly see a P-wave arrival and an S-wave arrival about 7 seconds later. The P-wave has a higher amplitude on the vertical component, and the S-wave has a higher amplitude on the horizontal components.

than 100 kilometers away from the epicenter of an LFE family, as the template would be unlikely to have a good signal-to-noise ratio. We then used this new, shorter templates for the permanent stations to make an LFE catalog for the period 2007-2009.

## 4  Results

Once we have obtained a catalog for the period 2007-2009 using the data from the permanent seismic networks, we compare the LFE detections between the two catalogs: the FAME catalog (obtained with data from the FAME experiment) and the networks catalog (obtained from data from the permanent networks). As we may have many false detections, we try to eliminate some of them by assuming that LFEs present in both catalogs are always true detections. Then we define two thresholds: the first threshold is chosen such that at least half the LFE detections above the threshold in the FAME catalog are also in the network catalog, the second threshold is chosen such that at least half the LFE detections above the threshold in the network catalog are also in the FAME catalog. If we filter the catalogs and keep only detections above the thresholds, we are now confident that at least half of the LFE detections are true detections. As the number of stations recording may vary over time (especially for the permanent networks catalog), we keep only the LFE detections such that the associated cross correlation multiplied by the number of channels recording at that time is higher than the threshold. Thus, if there are few stations recordings at some time, the cross correlation must be higher for the LFE to be considered as a true detection. We then compared the normalized number of LFEs obtained with the two catalogs. Examples are given in Figure 5 for families A (square in Figure 1) and E (inverted triangle in Figure 1). Although the number of LFEs during each **cluster of LFEs** may not be the same, we clearly see for family E that the timing of the events are the same for both catalogs. Family A has much shorter recurrence times but most **clusters of LFEs are present in both catalogs as well: forty clusters are present in both catalogs, three clusters are present in the FAME catalog but not in the networks catalog and one cluster is present in the networks catalog but not in the FAME catalog.**

For most of the families located on the subduction zone, we obtained a good agreement between both catalogs. We eliminate six families for which too few permanent stations have good templates, and it was not possible to detect LFEs with the available templates. However, we were able to detect most LFE events even without the presence of the temporary stations from the FAME network. We are thus confident that we can detect LFEs before 2007 and after 2009. In the following, we focus on the period 2004-2011. In November 2011, several one-component stations stopped recording and the number of available stations started decreasing, which is why we did not look for LFE events after that date. The resulting LFE catalog for the period 2004-2011 is shown in Figure 6.
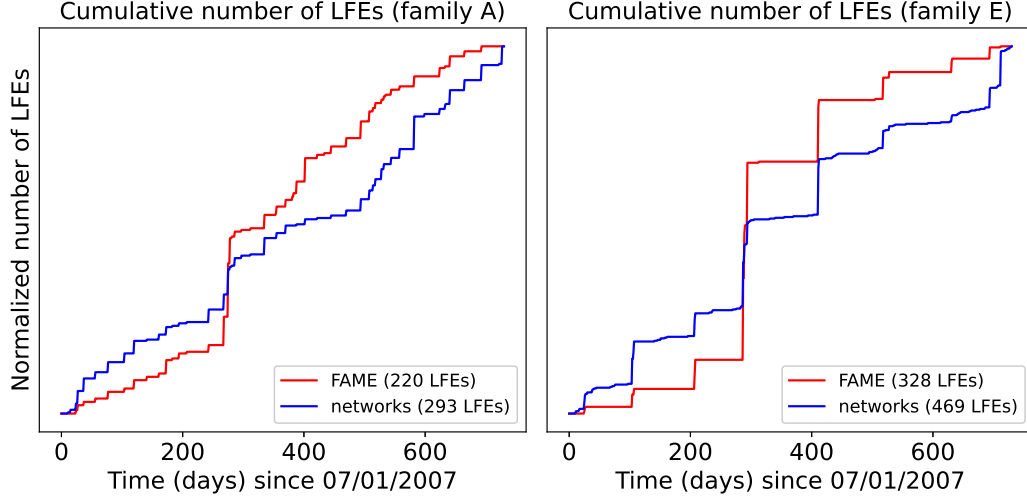
**Figure 5.** Normalized cumulative number of LFEs over the period July 2007-July 2009 for the FAME catalog (red) and the network catalog (blue) for family A (square in Figure 1) and family E (inverted triangle in Figure 1). The cumulative number of LFEs has been divided by the total number of LFEs so that both curves start at 0 and end at 1, in order to get a better match between the LFE bursts in both catalogs.

For comparison, we also plotted the tremor detection times from Boyarko et al. (2015). Figure 7 shows the details of six big ETS events in 2004, 2005, 2006, 2007 and 2008. **The catalog shown in Figure 6 has been filtered using the threshold computed above. Filtering the catalog has removed about 63 % of the LFEs, compared to the initial catalog where LFEs were detected using the 8 \* MAD threshold for the cross-correlation. As a reference, we plotted in the Supplementary Material (Figure S2) the catalog without filtering the LFEs and the number of channels recording as a function of time.**

## 5 Discussion

We were able to detect LFE events propagating from North to South or from South to North whenever there is a tremor episode in the Boyarko et al. (2015) catalog. We were also able to detect several LFE episodes in 2004-2005 before the beginning of the Boyarko et al. (2015) catalog. In particular, the LFE event in January 2005 propagating South to North from latitude 40.1 to latitude 41.2 is also present in the ETS catalog from Brudzinski and Allen (2007). We also see one LFE event in May-June 2004, propagating South to North from latitude 40.1 to 41.6, and one LFE event in November 2004, propagating North to South from latitude 41.6 to 40.4. The first of these events is also in the ETS catalog from Brudzinski and Allen (2007). The main characteristics of the six biggest events shown in Figure 7 are given in Table 1.

It is known than tectonic tremor can be triggered by surface waves from distant and regional earthquakes, as has been observed in Cascadia (Rubinstein et al., 2009), the San Andreas (Peng et al., 2009; Guilhem et al., 2010), and Nankai **(Miyazawa et al., 2008; Han et al., 2014)**. LFE activity on the San Andreas fault also increased during several months after the 2004 Parkfield earthquake (Shelly, 2017). We looked for regional earthquakes with magnitude higher than 5 during the period covered by the catalog to verify whether this phenomenon is also observed in southern Cascadia. The
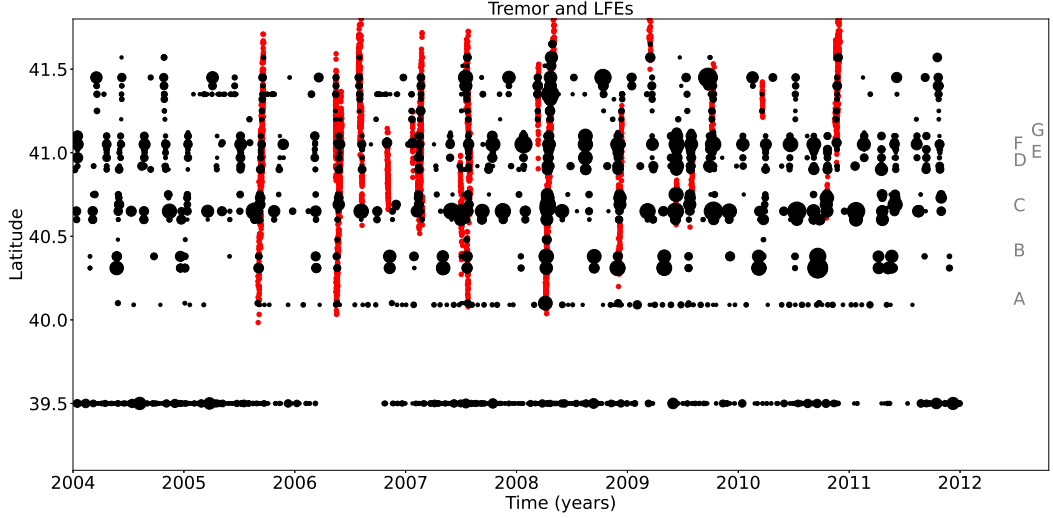
**Figure 6.** LFE and tremor detections as a function of time and latitude. Red dots represent tremor detections from the catalog of Boyarko et al. (2015). Black dots represent days where LFEs are detected for a given LFE family. The size of the black dots are proportional to the number of LFEs detected during this day. For clarity, we do not show the LFEs for the days when there are less than three LFEs.
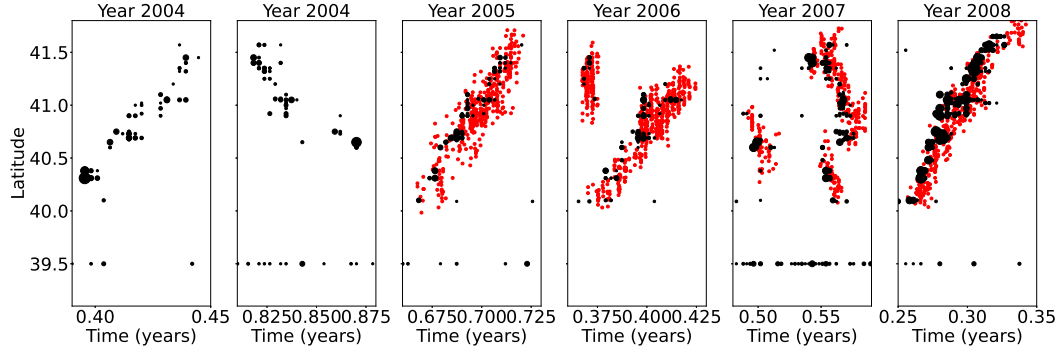


**Figure 7.** LFE and tremor detections as a function of time and latitude for six ETS events. Red dots represent tremor detections from the catalog of Boyarko et al. (2015). Black dots represent days where LFEs are detected for a given LFE family. The size of the black dots are proportional to the number of LFEs detected during this day. For clarity, we do not show the LFEs for the days when there are less than three LFEs. **The tremor catalog of Boyarko et al. (2015) starts in 2005. This is why no tremor detections can be shown for the two events in 2004.**

**Table 1.** Main LFEs events between 2004 and 2011

| Begin time | End time | Direction | Southern limit | Northern limit |
|---|---|---|---|---|
| End May 2004 | Mid June 2004 | South to North | 40.1 | 41.6 |
| Early November 2004 | End November 2004 | North to South | 40.4 | 41.6 |
| Early September 2005 | End September 2005 | South to North | 40.1 | 41.6 |
| Mid April 2006 | End April 2006 | South to North | 40.1 | 41.5 |
| Early July 2007 | End July 2007 | North to South | 40.1 | 41.6 |
| Early April 2008 | End April 2008 | South to North | 40.1 | 41.7 |

**Table 2.**   Nearby regional earthquakes between 2004 and 2011

| Magnitude | Time | Latitude | Longitude | Depth (km) |
|-----------|------|----------|-----------|------------|
| 7.2 | 2005-06-15 02:50:54 | 41.292N | 125.953W | 16.0 |
| 6.6 | 2005-06-17 06:21:42 | 40.773N | 126.574W | 12.0 |
| 6.5 | 2010-01-10 00:27:39 | 40.652N | 124.693W | 28.7 |
| 5.9 | 2010-02-04 20:20:21 | 40.412N | 124.961W | 23.0 |
| 5.4 | 2008-04-30 03:03:06 | 40.836N | 123.497W | 27.8 |
| 5.0 | 2006-07-19 11:41:43 | 40.281N | 124.433W | 20.1 |

**Table 3.**   Teleseismic earthquakes between 2004 and 2011

| Magnitude | Time | Latitude | Longitude | Depth (km) |
|-----------|------|----------|-----------|------------|
| 9.1 | 2011-03-11 05:46:24 | 38.297N | 142.373E | 29.0 |
| 9.1 | 2004-12-26 00:58:53 | 3.295N | 95.982E | 30.0 |
| 8.8 | 2010-02-27 06:34:11 | 36.122S | 72.898W | 22.9 |
| 8.6 | 2005-03-28 16:09:36 | 2.085N | 97.108E | 30.0 |
| 7.9 | 2008-05-12 06:28:01 | 31.002N | 103.322E | 19.0 |

characteristics of the earthquakes we looked at are given in Table 2. We also looked at distant earthquakes with large magnitude, which characteristics are given in Table 3.

Although we observe an increase in LFE activity for some families several days after the earthquakes (except the 2008 one where no activity is observed after the earthquake), it does not seem that this activity is linked to the earthquake. Indeed, the LFE events occur a few days after the earthquake and not immediately after as is the case for the Parkfield earthquake, and they affect only a few families. The reason may be due to the distance between the LFE families and the epicenters of the regional earthquakes. Indeed, for the Parkfield earthquake, an increase in LFE activity was observed for LFE families up to 45km away from the epicenter, but not farther away. Moreover, the Parkfield earthquake was more shallow (8.1km deep) than the regional earthquakes used in this study. For the 2003 M6.5 San Simeon earthquake, no increase in LFE activity in the San Andreas LFE families was observed in the hours following the earthquake. This was also a shallow earthquake (8.4km deep) but the epicenter was farther away from the LFE families (60 to 100 km). For southern Cascadia, the closest epicenter (2008) is located 50 km away from the closest LFE families. Based on what was observed for the San Andreas LFE families, this distance may be too large for a regional earthquake to trigger an increase in LFE activity. We do not see any change in LFE activity after the large teleseismic earthquakes. There was not any change in LFE activity for the San Andreas LFE families either.

In northern Cascadia, it has been observed that there is an increase in activity downdip of the plate boundary compared to up dip, both for tremor (Wech & Creager, 2011) and LFEs (Sweet et al., 2019). We want to verify whether we can see an increase of LFE activity for the downdip LFE families compared to the updip LFE families. Most families in the northern and central part of the study area are well aligned along the strike direction, however families in the southern part of the subduction zone are more distant from each other. We first look at three families aligned at latitude about 40.4N (group B, triangles in Figure 1) and show the number of LFEs per day in the left column of Figure 8. We then look at five families aligned at latitude about 40.7N (group C, diamonds in Figure 1) and show the number of LFEs per day in the middle column of Figure 8. Finally, we look at five families aligned at latitude about 41.05N (group G, pentagons in Figure 1) and show the number of LFEs per day in the right column of Figure 8. For
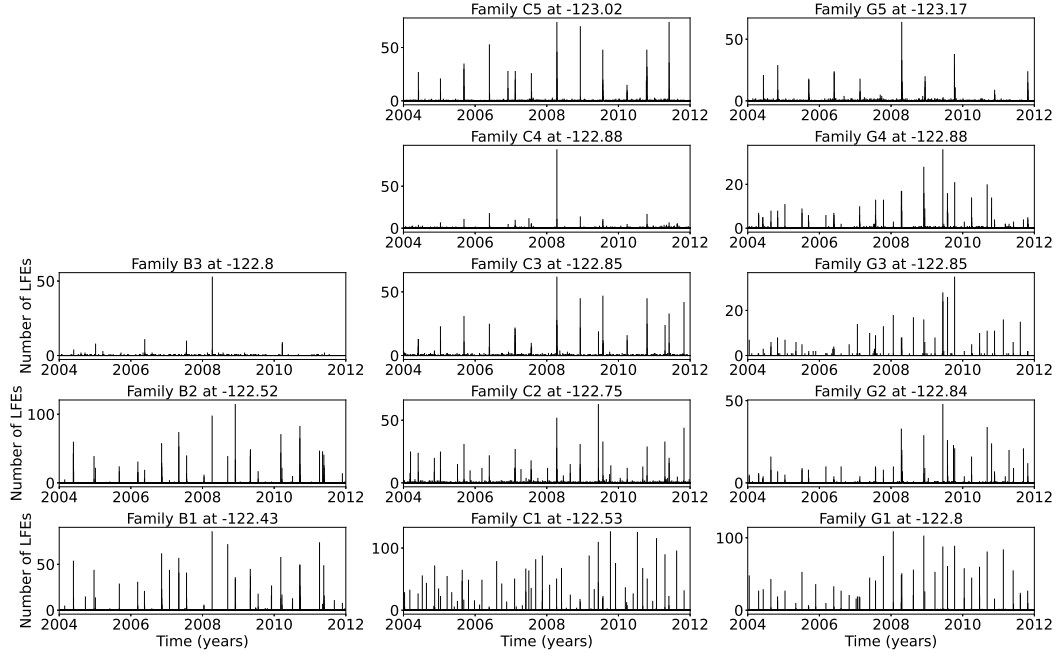
**Figure 8.** Left: Daily number of LFEs over the period 2004-2011 for the three LFE families in group C (triangles in Figure 1). Middle: Daily number of LFEs for the five LFE families in group D (diamonds in Figure 1). Right: Daily number of LFEs for the five LFE families in group E (pentagons in Figure 1). Down-dip families (lower rows) typically have far more LFE swarms that up-dip families (upper rows).

all three sets of families, LFE events are more frequent for the easternmost family than for the westernmost family, as was also the case in northern Cascadia (Sweet et al., 2019). It is more difficult to compare event size and swarm duration as the number of stations and the quality of the templates are different for each family, and may have a strong influence on the number of LFEs detected. To summarize the findings, we plot in Figure 9 the **average time between** LFE events as a function of the distance in the eastern direction from the **western** limit of the tremor. **We assume that there is an LFE event avery time that at least five LFEs are recorded during a given day. If two events are separated by less than five days, we assume that this is a single event.** We clearly see that the **average time between LFE events** decreases with the down dip distance. The southernmost family A is also added in Figure 9, but does not fit the general trend.

The occurrence and amplitude of tectonic tremor can be modulated by small stress changes (about 1 kPa) associated with ocean or solid earth tides **(Shelly et al., 2007b; Houston et al., 2011; Houston, 2015)**. Sensitivity of LFE families activity to tidal stress changes has also been observed in northern Cascadia (Royer et al., 2015), and on the San Andreas fault (Thomas et al., 2012). We used calculated stresses from elastic deformations due to both water loads and body tides in the solid Earth along the Cascadia subduction zone. The stress computation is done following the method described in Houston (2015). The resulting full stress tensors are projected to normal and shear (in the plate convergence direction) stresses on the interface, as well as mean stress (one-third the tensor trace). The change in Coulomb stress (positive promotes shear failure) $\Delta CFF$ is then computed:
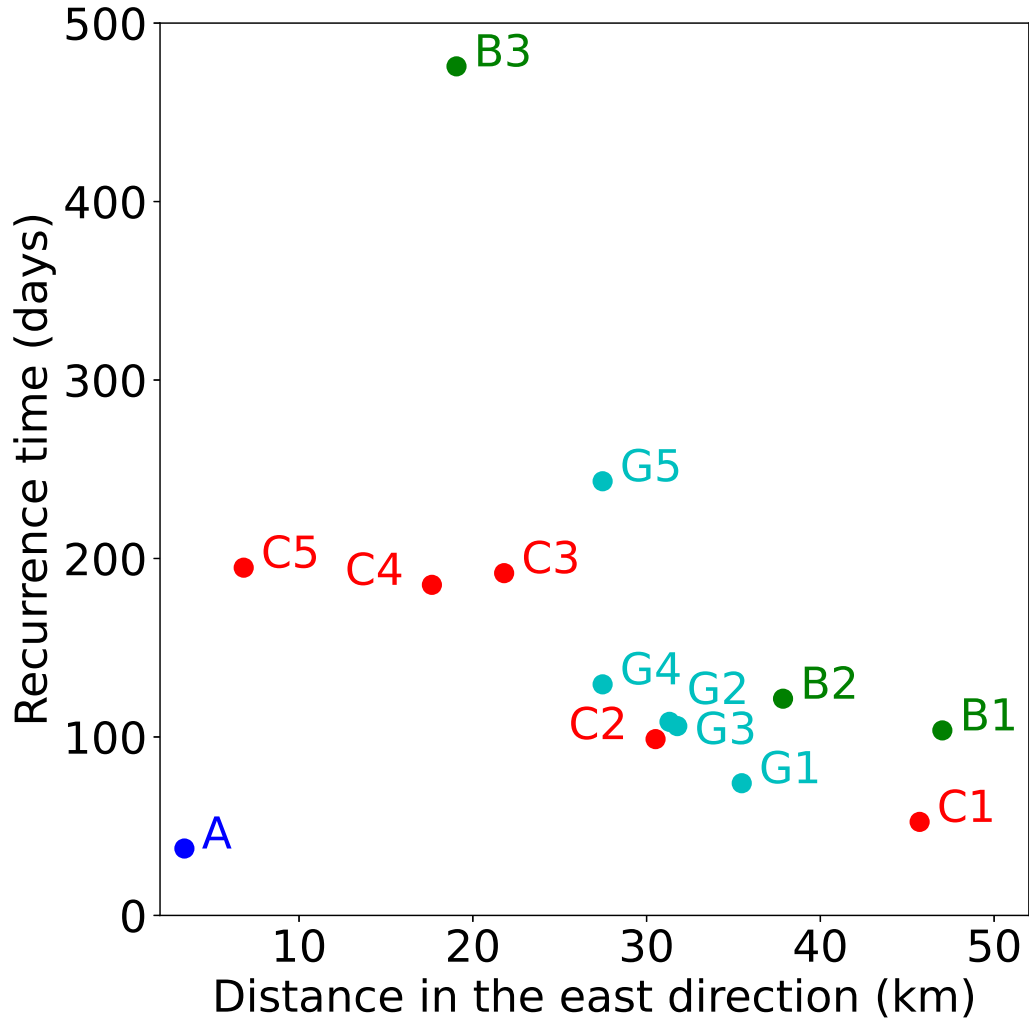
**Figure 9.** **Average time between** LFE events as a function of distance in the eastern direction from the **westward** limit of tremor for the three LFE families in group B (triangles in Figure 1), the five LFE families in group C (diamonds in Figure 1), and the five LFE families in group G (pentagons in Figure 1). Family A (square in Figure 1) has much **shorter time intervals between** LFE events.
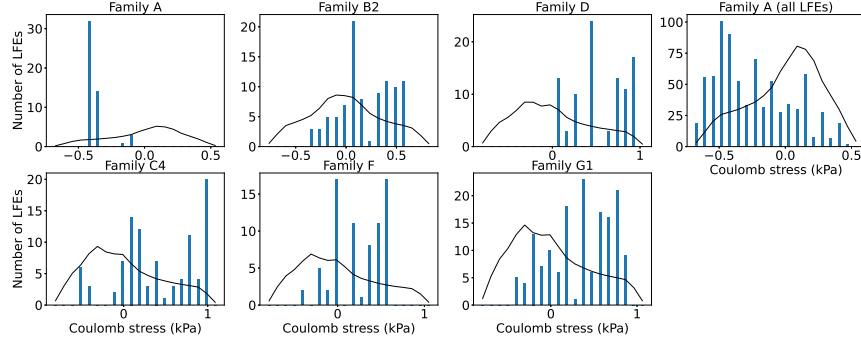
**Figure 10.** Number of LFEs for families A, B2, D, C4, F and G1 observed (blue bars) and expected (black line) for each stress bin of tidal Coulomb stress change.

$$\Delta CFF = \Delta\tau + \mu\left(\Delta\sigma - B\Delta\sigma_m\right) \tag{1}$$

where $\Delta\tau$ is the change in shear stress on the fault plane in the slip direction, $\Delta\sigma$ is the change in fault normal stress (positive is tensile), $\mu$ is the coefficient of intrinsic friction, $\Delta\sigma_m$ is the change in mean stress and $B$ is the Skempton's coefficient (Houston, 2015). We take the values $\mu = 0.1$ and $B = 0.5$ for the friction and the Skempton's coefficient, **as was done by Houston (2015)**. We then divided the values of tidal Coulomb stress change into 20 stress bins and computed for each LFE family the number of LFEs occurring at a time when the value of the stress was in a given bin. We also computed what would be the expected number of LFEs occurring if the tidal stress changes have no influence on LFE activity. As noted by Houston (2015), tremor sensitivity to stress perturbations changes during an ETS event, with an increase in sensitivity to tidal stress as slip accumulates over several days. We thus choose to only consider the later part of the 2008 ETS event, using only LFEs that occurred between 1.5 and 11.5 days after the arrival of the tremor front. As there are only a few LFEs, it is not always obvious to see the influence of tidal stress on LFE activity. However, Figure 10 shows the number of LFEs occurring during each stress bin (blue bars) and the expected number of LFEs (black line) for six families with a relatively high number of LFEs. For most of the families, a positive Coulomb stress change (promoting shear failure) is associated with an increase in LFE activity. However, this is not the case for the southernmost LFE family A, for which a negative Coulomb stress change is associated with an increase in LFE activity. To better highlight the behavior of family A, we also consider the whole LFE catalog and plot the observed and expected number of LFEs as a function of tidal stress. We clearly see that these LFEs tend to occur during times when predicted tidal Coulomb stress is discouraging slip on the plate boundary. We hypothesize that LFE family A may not be located on the subduction zone, and may be on a different fault instead.

## 6 Conclusion

In this study, we used the templates obtained by Plourde et al. (2015) using data recorded by the FAME network in Northern California during an episode of high tremor activity in April 2008, and we extended their catalog to the whole two years (2007-2009) during which the seismic stations were installed. We then used the two-year-long catalog to create templates for stations from the permanent seismic networks, and used the seismic data recorded by these stations to extend the catalog before and after the FAME experiment. We observe LFEs every time that there is tectonic tremor on the tremor cat-

alog from Boyarko et al. (2015), and several additional smaller LFE episodes. Whereas
the LFE families from the subduction zone are mainly active during the big Episodic Tremor
and Slip events, the southernmost family is more active, with repeating events about once
a month. Downdip families are also more active than up dip families. Tidal stress changes
seem to be correlated with LFE activity in the later part of the 2008 ETS event.

### References

Audet, P., & Kim, Y. H. (2016). Teleseismic constraints on the geological environ-
    ment of deep episodic slow earthquakes in subduction zone forearcs: A review.
    *Tectonophysics*, *670*, 1-15.

Baratin, L. M., Chamberlain, C. J., Townend, J., & Savage, M. K. (2018). Focal
    mechanisms and inter-event times of low-frequency earthquakes reveal quasi-
    continuous deformation and triggered slow slip on the deep Alpine Fault. *Earth
    and Planetary Science Letters*, *484*, 111-123.

Beroza, G. C., & Ide, S. (2011). Slow earthquakes and nonvolcanic tremor. *Annu.
    Rev. Earth Planet. Sci.*, *39*, 271-296.

Bostock, M. G., Royer, A. A., Hearn, E. H., & Peacock, S. M. (2012). Low fre-
    quency earthquakes below southern Vancouver Island. *Geochemistry Geo-
    physics Geosystems*, *13*, Q11007.

Bostock, M. G., Thomas, A. M., Savard, G., Chuang, L., & Rubin, A. M. (2015).
    Magnitudes and moment-duration scaling of low-frequency earthquakes be-
    neath southern Vancouver Island. *Journal of Geophysical Research: Solid
    Earth*, *120*, 6329-6350.

Boyarko, D. C., Brudzinski, M. R., Porritt, R. W., Allen, R. M., & Tréhu, A. M.
    (2015). Automated detection and location of tectonic tremor along the entire
    Cascadia margin from 2005 to 2011. *Earth and Planetary Science Letters*, *430*,
    160-170.

Brudzinski, M. R., & Allen, R. M. (2007). Segmentation in episodic tremor and slip
    all along Cascadia. *Geology*, *35*(10), 907-910.

Chestler, S. R., & Creager, K. C. (2017a). Evidence for a scale-limited low-frequecny
    earthquake source process. *Journal of Geophysical Research: Solid Earth*, *122*,
    3099-3114.

Chestler, S. R., & Creager, K. C. (2017b). A model for low-frequency earthquake
    slip. *Geochemistry, Geophysics, Geosystems*, *18*, 4690-4708.

Ducellier, A. (2021, August). *Arianeducellier/catalog: Paper submission.* Zen-
    odo. Retrieved from https://doi.org/10.5281/zenodo.5168867 doi: 10

.5281/zenodo.5168867

Frank, W. B., Shapiro, N. M., Husker, A. L., Kostoglodov, V., Romanenko, A., & Campillo, M. (2014). Using systematically characterized low-frequency earthquakes as a fault probe in Guerrero, Mexico. *Journal of Geophysical Research: Solid Earth*, *119*, 7686-7700.

Guilhem, A., Peng, Z., & Nadeau, R. M. (2010). High-frequency identification of non-volcanic tremor triggered by regional earthquakes. *Geophysical Research Letters*, *37*, L16309.

Han, J., Vidale, J. E., Houston, H., Chao, K., & Obara, K. (2014). Triggering of tremor and inferred slow slip by small earthquakes at the Nankai subduction zone in southwest Japan. *Geophysical Research Letters*, *41*, 8053-8060.

Houston, H. (2015). Low friction and fault weakening revealed by rising sensitivity of tremor to tidal stress. *Nature Geoscience*, *8*(5), 409-415.

Houston, H., Delbridge, B. G., Wech, A. G., & Creager, K. C. (2011). Rapid tremor reversals in Cascadia generated by a weakened plate interface. *Nature Geoscience*, *4*, 404-409.

Ide, S., Shelly, D. R., & Beroza, G. C. (2007). Mechanism of deep low frequency earthquakes: Further evidence that deep non-volcanic tremor is generated by shear slip on the plate interface. *Geophysical Research Letters*, *34*, L03308.

Kato, A., & Nakagawa, S. (2020). Detection of deep low-frequency earthquakes in the Nankai subduction zone over 11 years using a matched filter technique. *Earth, Planets and Space*, *72*, 128.

Katsumata, A., & Kamaya, N. (2003). Low-frequency continuous tremor around the Moho discontinuity away from volcanoes in the southwest Japan. *Geophysical Research Letters*, *30*(1), 1020.

Levander, A. (2007). *Seismic and geodetic investigations of mendocino triple junction dynamics.* International Federation of Digital Seismograph Networks. Retrieved from `https://www.fdsn.org/networks/detail/XQ_2007/` doi: 10.7914/SN/XQ_2007

McCrory, P. A., Blair, J. L., Oppenheimer, D. H., & Walter, S. R. (2006). *Depth to the Juan de Fuca slab beneath the Cascadia subduction margin - a 3-D model sorting earthquakes* (Tech. Rep. No. Data Series 91). U.S. Geological Survey.

Miyazawa, M., Brodsky, E. E., & Mori, J. (2008). Learning from dynamic triggering of low-frequency tremor in subduction zones. *Earth, Planets and Space*, *60*, e17-e20.

Nakamura, M. (2017). Distribution of low-frequency earthquakes accompanying the very low frequency earthquakes along the Ryukyu Trench. *Earth, Planets, and Space*, *69*(1), 1-17.

Obara, K. (2002). Nonvolcanic deep tremor associated with subduction in southwest Japan. *Science*, *296*(5573), 1679-1681.

Obara, K., Hirose, H., Yamamizu, F., & Kasahara, K. (2004). Episodic slow slip events accompanied by non-volcanic tremors in southwest Japan subduction zone. *Geophysical Research Letters*, *31*, L23602.

Ohta, K., & Ide, S. (2017). Resolving the detailed spatiotemporal slip evolution of deep tremor in Western Japan. *Journal of Geophysical Research: Solid Earth*, *122*(12), 10009-10036.

Peng, Z., Vidale, J. E., Wech, A. G., Nadeau, R. M., & Creager, K. C. (2009). Remote triggering of tremor along the San Andreas Fault in central California. *Journal of Geophysical Research*, *114*, B00A06.

Plourde, A. P., Bostock, M. G., Audet, P., & Thomas, A. M. (2015). Low-frequency earthquakes at the southern Cascadia margin. *Geophysical Research Letters*, *42*, 4849-4855.

Rogers, G., & Dragert, H. (2003). Tremor and slip on the Cascadia subduction zone: The chatter of silent slip. *Science*, *300*(5627), 1942-1943.

Royer, A. A., & Bostock, M. G. (2014). A comparative study of low frequency earth-

quake templates in northern Cascadia. *Earth and Planetary Science Letters*, *402*, 247-256.

Royer, A. A., Thomas, A. M., & Bostock, M. G. (2015). Tidal modulation and triggering of low-frequency earthquakes in northern Cascadia. *Journal of Geophysical Research Solid Earth*, *120*, 384-405.

Rubinstein, J. L., Gomberg, J., Vidale, J. E., Wech, A. G., Kao, H., Creager, K. C., & Rogers, G. (2009). Seismic wave triggering of nonvolcanic tremor, episodic tremor and slip, and earthquakes on Vancouver Island. *Journal of Geophysical Research Solid Earth*, *114*, B00A01.

Shelly, D. R. (2017). A 15 year catalog of more than 1 million low-frequency earthquakes: Tracking tremor and slip along the deep San Andreas Fault. *Journal of Geophysical Research: Solid Earth*, *122*, 3739-3753.

Shelly, D. R., Beroza, G. C., & Ide, S. (2007a). Non-volcanic tremor and low-frequency earthquake swarms. *Nature*, *446*, 305-307.

Shelly, D. R., Beroza, G. C., & Ide, S. (2007b). Complex evolution of transient slip derived from precise tremor locations in western Shikoku, Japan. *Geochemistry, Geophysics, Geosystems*, *8*, Q10014.

Shelly, D. R., Beroza, G. C., Ide, S., & Nakamula, S. (2006). Low-frequency earthquakes in Shikoku, Japan, and their relationship to episodic tremor and slip. *Nature*, *442*, 188-192.

Sweet, J. R., Creager, K. C., Houston, H., & Chestler, S. R. (2019). Variations in Cascadia low-frequency earthquake behavior with downdip distance. *Geochemistry, Geophysics, Geosystems*, *20*, 1202-1217.

Thomas, A. M., Bürgmann, R., Shelly, D. R., Beeler, N. M., & Rudolph, M. L. (2012). Tidal triggering of low frequency earthquakes near Parkfield, California: Implications for fault mechanics within the brittle-ductile transition. *Journal of Geophysical Research*, *117*, B05301.

Wech, A. G., & Creager, K. C. (2011). A continuum of stress, strength and slip in the Cascadia subduction zone. *Nature Geoscience*, *4*, 624-628.

Wessel, P., & Smith, W. H. F. (1991). Free software helps map and display data. *EOS Trans. AGU*, *72*, 441.